THIELE CENTRE
FOR APPLIED MATHEMATICS IN NATURAL SCIENCE

Modelling resting state networks in the human brain

Thordis L. Thorarinsdottir and Eva B. Vedel Jensen

Research Report

No. 10 | June 2006

Modelling resting state networks in the human brain

This Thiele Research Report is also Research Report number 479 in the Stochastics Series at Department of Mathematical Sciences, University of Aarhus, Denmark.

Modelling resting state networks in the human brain

Thordis L. Thorarinsdottir[*,**], Eva B. Vedel Jensen[**]

Abstract

In the present paper, we show how spatio-temporal point process models for functional magnetic resonance imaging (fMRI) data can be used in the study of resting state networks in the human brain. The model explicitly includes knowledge of the hemodynamic response to neuronal activation. Fully Bayesian analysis of the model is described and an example of analysis of a fMRI data set is given. Other methods of analysis of resting state networks are also discussed.

Keywords: Bayesian inference, fMRI, hemodynamic response function, Markov chain Monte Carlo, spatio-temporal point processes

1 Introduction

Cognitive psychologists and neuroscientists are presently very interested in the functioning of the human brain during rest. One of the reasons is that analyses of data obtained by functional magnetic resonance imaging (fMRI) indicate the existence of resting state networks of regions in the human brain, cf. [3, 7, 8, 15] and references therein. See also the collection of papers presented in the special issue of *Phil. Trans. R. Soc.* from 2005 on 'Multimodal neuroimaging of brain connectivity'. Changes of these networks under aging or disease have been reported ([5], [15]).

During an fMRI experiment the brain is scanned and represented as a set of voxels. At each voxel a time series of MR signal intensities is recorded, showing the local brain activity during the experiment. Time series from regions far apart may show similar variation during rest, indicating the presence of a resting state network. An example of such data, earlier analyzed in [3], is shown in Fig. 1. At each voxel of a slice through the human brain, the MR signal intensity is shown at 12 equidistant time points of the scanning experiment. The person being scanned here has not received any particular stimuli during the experiment but still covariation between activities in different regions of the brain may appear. As we shall see, there is evidence of covariation between activities in the three regions shown in Fig. 3 below, but this is not immediate from Fig. 1. We will return to this example at the end of the paper. Generally, modelling and statistical analysis of such data

[*]The MR Centre, Skejby University Hospital, University of Aarhus, Denmark (disa@imf.au.dk)
[**]The T.N. Thiele Centre for Applied Mathematics in Natural Science, Department of Mathematical Sciences, Ny Munkegade, DK-8000 Aarhus C, Denmark (eva@imf.au.dk)

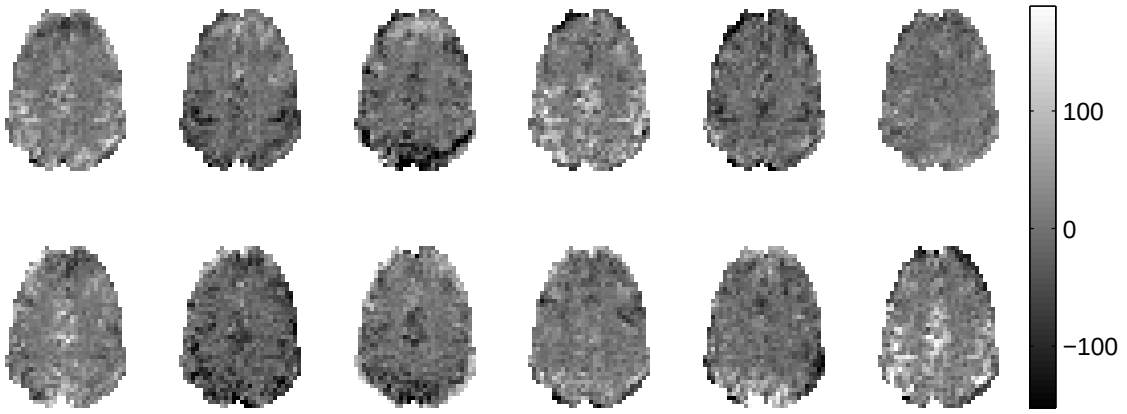

Figure 1: Development of the MR signal activity over time in a single slice through the human brain. From left to right and top to bottom: the activity at time $t = 12, 30, 48, \ldots, 210$ seconds.

constitute a major challenge because of a high level of noise and no prior knowledge of time points of activation. Another complication is possible aliasing with respiratory and cardiac cycles. The difficulties faced in such non-stimulus experiments are much more serious than those met in more traditional experimental designs of fMRI experiments with known periods of stimuli ('on periods') between periods of rest ('off periods'). Recently, experiments with a more continuous but known type of stimulus has also been tried out, cf. [1, 2]. A good statistical review on design of fMRI experiments may be found in [10].

The aim of this paper is to show how spatio-temporal point process models for functional magnetic resonance imaging (fMRI) data can be used in the study of resting state networks in the human brain. A more detailed account will be published elsewhere [19].

2 Correlation analysis

The data from an fMRI experiment constitute a collection of time series

$$Z_{tx}, \quad t = t_1, \ldots, t_m,$$

$x \in \mathcal{X}$. Here, Z_{tx} is the MR signal intensity at time t and voxel x. The time points $t_1, \ldots, t_m$ are usually equidistant and belong to the interval $[0, T]$, where T is the length of the experiment. The set $\mathcal{X}$ is a finite subset of $\mathbb{R}^2$ or $\mathbb{R}^3$ with N elements, called voxels, representing a two dimensional slice or a three dimensional volume of the brain.

In [8], the functional connectivity in the resting brain is studied by a simple correlation analysis. A seed region $\mathcal{X}_0 \subset \mathcal{X}$ is selected and the correlation between the average time series for this region

$$\bar{Z}_{t\mathcal{X}_0} = \frac{1}{|\mathcal{X}_0|} \sum_{x \in \mathcal{X}_0} Z_{tx}, \quad t = t_1, \ldots, t_m$$

and the time series of any other brain voxel is calculated in order to find regions $\mathcal{X}_1$ interacting with $\mathcal{X}_0$. Here, $|\cdot|$ indicates number. Similarly, in [13], the average time series is used as explanatory variable in a regression type of analysis of the time variation in other regions of the brain. The software package SPM (Statistical Parametric Mapping), developed by the Wellcome Department of Imaging Neuroscience, UCL, UK, can be used for such an analysis.

This analysis is attractive because it is simple. It does, however, require an a priori expectation of the network pattern.

3 Independent component analysis

Independent component analysis (ICA) has become a very popular technique for analyzing data from fMRI experiments without specific stimuli. A number of interesting findings relating to specific resting state networks have been reported using ICA ([3, 14, 15]). A special variant of the technique is called probabilistic independent component analysis (PICA), cf. [7]. There were some early critiques of ICA, see [9], but it seems now to be generally recognized in the neuroscience community that ICA is a powerful nonparametric tool for studying resting state networks. A good introduction to ICA can be found in [21]. This paper also contains a comprehensive list of references with specific guidance to the literature. Analysis of groups of individuals by ICA is discussed in [4].

ICA is an explorative analysis, closely related to factor analysis and discriminant analysis. The analysis is based on a model of the following type

$$Z_{tx} = \mu_x + \sum_{k=1}^{K} A_{tk} B_{kx} + \sigma \epsilon_{tx}.$$

Here, μ_x is the baseline signal at voxel x which can vary by a factor of 2-3 across the brain. The number K of components is unknown. Furthermore, $(A_{\star k}, B_{k\star})$, $k = 1, \ldots, K$, are assumed to be independent. Software packages performing ICA are available, e.g. the program FSL presented in [25]. An ICA analysis results in estimates of temporal activation profiles $\{A_{\star k}\}$ and spatial activation profiles $\{B_{k\star}\}$ for each k. The estimated temporal profiles are shown together with their associated power spectra. Only frequency components of a certain bandwidth are regarded as having neuronal origin. High frequence components may be caused by cardiac or respiratory activities, while very low frequence components are considered to be drift. In an actual application, the estimated number K of components may be quite large.

4 A model based on spatio-temporal point processes

Especially amongst psychologists, there has recently been some criticism of ICA analysis because such an analysis decomposes a particular type of activity in the brain into a spatial activation map showing regions of the brain activated during the

experiment and a temporal activation graph showing when the brain is activated during the experiment. They are not particularly fond of this type of 'product brain'. Instead, a more dynamic type of analysis is asked for in order to be able to reveal more complicated interaction phenomenon. For instance, a particular region of the brain may only be active if a collection of other regions are active. An example of this is the visual system which seems to have a very strong hierarchical structure, see [17]. It may also be of interest to investigate whether the duration and extend of activation may depend on the particular region of the brain studied. As we shall see, this criticism can be met by using a spatio-temporal point process modelling approach.

The model to be presented depends on well established knowledge on the hemodynamic response which is a localized inflow of oxygenated blood to a region of the brain with neural activity. This response causes an increase of the MR signal intensity in the region in question. Its general temporal form has been reproduced in many studies. First, the hemodynamic response increases to a peak value at about 4–7 seconds after a neuronal response and then it returns to baseline again a few seconds after the neuronal impulse has ceased.

A neuronal activation at location y and time u will therefore contribute to the observed MR signal intensity at y at the later time $t > u$ by an amount proportional to

$$g(t-u)$$

where g is a function with the properties described above. In particular, $g(v)$ increases to a maximal value for v equal to 4-7 seconds and then decreases to 0 after the neuronal activation has stopped. A neuronal activity in voxel y is expected to affect the activity at neighbour voxels in a similar way but less intensely. For a voxel x, an activation at location y and time u will contribute to the observed MR signal intensity at x at the later time $t > u$ by the following amount

$$g(t-u)h(x-y),$$

where $h(z)$ is a decreasing function of $\|z\|$. The resulting model for the contribution to the observed MR signal intensity at voxel x at time t caused by a neuronal activation at voxel y at time u becomes

$$f_{tx}(u, y; m) = g(t-u; m^1)h(x-y; m^2)$$

where $m = (m^1, m^2)$ and m^1 and m^2 are model parameters, describing the duration of a neuronal activation and its spatial extent.

The actual modelling of the hemodynamic response function g has been studied intensively in the fMRI literature, see [6] and references therein. We will here adopt a fairly simple but well-known model where the response is a Gaussian distributed random variable with mean 6 sec (the delay) and variance 9 sec^2. Accordingly, the function g takes the form

$$g(u; m^1) = \int_0^{m^1} \kappa(u-v)dv,$$

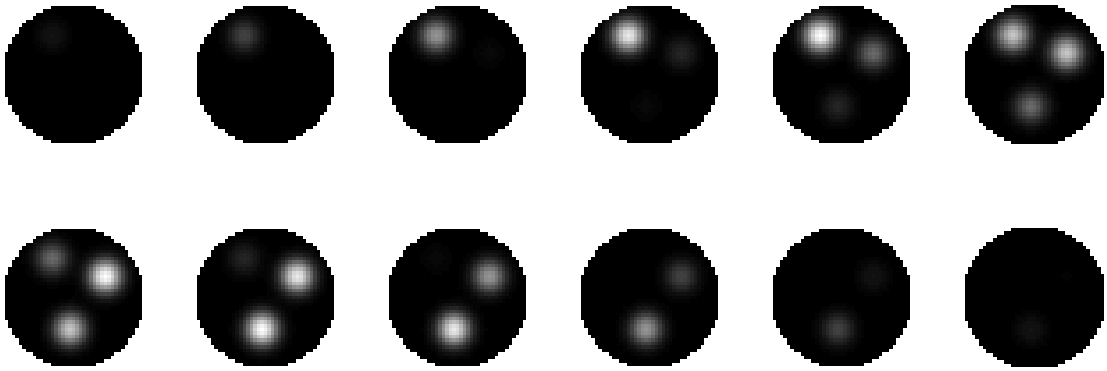

Figure 2: Development of the activity over time in simulated data. From left to right and top to bottom: the activity at time $t = 2, 4, \ldots, 24$ time units. The activity starts at times $t = 1, 6, 8$, clockwise from the top, and the marks are given by $m^1 = 5$ time units and $m^2 = (10, 10)$ voxel units. The diameter of the circular disc is 40 voxel units. For more details, see the text.

where l is the temporal duration of the neuronal activation and

$$\kappa(t) = \frac{1}{\sqrt{2\pi}3} \exp\left(-\frac{(t-6)^2}{18} \right).$$

The spatial activation function is modelled by a Gaussian bell function

$$h(y; m^2) = \theta_1 \exp\left(-\frac{\|y\|^2}{2\theta_2} \right),$$

where $m^2 = (\theta_1, \theta_2)$.

In Fig. 2, we show the effect of superposition of three such activations. Here, $\mathcal{X}$ is a digitized circular disc. The activation profile

$$\Big\{ \sum_{i=1}^{3} f_{tx}(t_i, x_i; m) : x \in \mathcal{X} \Big\}$$

is shown for 12 equidistant time points. The time points and positions of the three activations (t_i, x_i), i=1, 2, 3, are indicated in the legend of Fig. 2. The duration m^1 and the spatial extent m^2 are the same for all three activations.

In an fMRI experiment without specific stimuli, the activations occur at random time points not known to the experimenter. It is natural to describe the activations by a marked point process $\Psi = \{[t_i, x_i; m_i]\}$ on $\mathbb{R} \times \mathcal{X}$ with marks $m_i = (m_i^1, m_i^2) \in \mathbb{R}_+^3$. The resulting model for the observed MR signal intensity at time t and voxel x becomes

$$Z_{tx} = \mu_x + \sum_i f_{tx}(t_i, x_i; m_i) + \sigma \epsilon_{tx}, \tag{1}$$

where μ_x is the baseline signal at voxel x as above and ϵ_{tx} is an error term with mean 0 and variance 1. The errors are expected to be correlated, see [20, 26]. It can be shown that this spatio-temporal model is closed under local smoothing, cf. [19].

Since the brain is not subjected to systematic stimuli under the fMRI experiment, it is natural to assume (investigate) that the marked point process Ψ is time stationary in the sense that

$$\Psi_t = \{[t_i + t, x_i; m_i]\}$$

has the same distribution as Ψ for all $t \in \mathbb{R}$. Then, the intensity measure Λ of the unmarked point process is of the form

$$\Lambda = c\nu^1 \times \Lambda_2,$$

where $c > 0$, ν^1 is the Lebesgue measure on $\mathbb{R}$ and Λ_2 is the intensity measure for the spatial point process $\{x_i\}$. Furthermore, time stationarity implies that the mark distribution does not depend on the particular time point considered but it may still depend on the location.

Under the resting state network hypothesis, the spatio-temporal point process Ψ will show long-distance dependencies. Recall that each marked point $[t_i, x_i; m_i]$ may be considered as a center of activation at location $x_i \in \mathcal{X}$ starting at time t_i and with temporal and spatial duration described by m_i. If two regions of the brain $\mathcal{X}_0$ and $\mathcal{X}_1$ interact, it is expected that activations occur almost simultaneously in $\mathcal{X}_0$ and $\mathcal{X}_1$. Such interactions may be revealed, using a ayesian analysis, see Section 5 below. The earlier modelling of a 'product brain' corresponds to the use of independent spatial and temporal point processes such that

$$\Psi = \{[t_i, x_j; m_i^1, m_j^2]\},$$

where $\Psi_1 = \{[t_i; m_i^1]\}$ and $\Psi_2 = \{[x_j; m_j^2]\}$ are independent. If the intensity measure of Ψ_2 is very concentrated in $\mathcal{X}_0$ and $\mathcal{X}_1$, then activations will appear simultaneously in the two regions. This type of modelling of the dependency may appear somewhat simplistic and a model based on conditional independence may be more natural. Here,

$$\Psi = \{[t_i, x_{ij}; m_i^1, m_{ij}^2]\},$$

where, given $\Psi_1 = \{[t_i; m_i^1]\}$, $\Psi_{2i} = \{[x_{ij}; m_{ij}^2]\}$ are independent and identically distributed with an intensity measure concentrated in $\mathcal{X}_0$ and $\mathcal{X}_1$, say.

In accordance with the emerging belief of the existence of more than one resting state network, it is natural to consider a point process model of the type $\Psi = \bigcup_{k=1}^K \Psi_k$ where $\Psi_k, k = 1, \ldots, K$, are independent and refer to activities in the K networks. If

$$\Psi_k = (\Psi_{k1}, \Psi_{k2})$$

where $\Psi_{k1} = \{[t_{ki}; m_{ki}^1]\}$ and $\Psi_{k2} = \{[x_{kj}; m_{kj}^2]\}$ are independent, then we obtain the following model equation

$$Z_{tx} = \mu_x + \sum_{k=1}^K A_{tk} B_{kx} + \sigma\epsilon_{tx}, \tag{2}$$

where

$$A_{tk} = \sum_i g(t - t_{ki}; m_{ki}^1) \text{ and } B_{kx} = \sum_j h(x - x_{kj}; m_{kj}^2).$$

Note that (2) is actually an ICA model. The model may be analyzed by first performing an ICA analysis and then analyzing the estimated components, using point process theory.

In the next section we will discuss Bayesian inference of the spatio-temporal point process model (1) and its parameters. A related model for repeated stimulus experiments has been developed in [16], see also [12].

5 Bayesian inference

5.1 Prior distributions

Without loss of generality we can set $\mu_x = 0$ in the following. The prior distribution of Ψ will be that of a Poisson point process. A typical point will, for convenience, be written as $[t, x; (\theta_0, \theta_1, \theta_2)] \in \mathbb{R} \times \mathcal{X} \times \mathbb{R}^3_+$ so we write here θ_0 instead of m^1 for the temporal duration of the neuronal activation. The intensity function of Ψ is assumed to be of the form

$$\lambda_\Psi(t, x; \theta_0, \theta_1, \theta_2) = \lambda(t, x) \prod_{i=0}^{2} \mathbf{1}\{\theta_i \in [a_i, b_i]\},$$

where a_i, b_i, $i = 0, 1, 2$, are known positive constants. Note that there is no interaction between points in this prior distribution so interactions will appear in the posterior distribution if they are present in the data.

We consider the restriction Ψ_0 of Ψ to

$$\mathcal{Y} = [T_{0-}, T_{0+}] \times \mathcal{X} \times \prod_{i=0}^{2} [a_i, b_i],$$

where the interval $[T_{0-}, T_{0+}]$ has been chosen such that an activation occurring outside this interval is very unlikely to affect the MR signal observed in $[0, T]$. The density of Ψ_0 with respect to the unit rate Poisson point process on $\mathcal{Y}$ becomes

$$\begin{aligned} p(\psi_0|\lambda, a_*, b_*) = \; & \exp\Big(- \prod_{i=0}^{2} (b_i - a_i) \int_{[T_{0-}, T_{0+}] \times \mathcal{X}} [\lambda(t, x) - 1] dt dx \Big) \\ & \times \prod_{[u,y;\theta_0,\theta_1,\theta_2] \in \psi_0} \Big[\lambda(u, y) \prod_{i=0}^{2} \mathbf{1}\{\theta_i \in [a_i, b_i]\} \Big]. \end{aligned}$$

We will model the function λ by a piecewise constant function only depending on location, i.e.

$$\lambda(t, x) = \sum_{l=1}^{K} \lambda_l \mathbf{1}\{x \in \mathcal{X}_l\}.$$

Here, the disjoint sets $\mathcal{X}_l$ are supposed to be specified by the experimenter while the parameters λ_l are unknown. The union of the sets $\mathcal{X}_l$ need not be the whole brain. We can write the intensity function as

$$\lambda(t, x) = c\lambda_2(x)$$

where $c > 0$ and

$$\int_{\mathcal{X}} \lambda_2(x)dx = 1.$$

Note that λ_2 is on the following form

$$\lambda_2(x) = \sum_{l=1}^{k} \pi_l \frac{\mathbf{1}\{x \in \mathcal{X}_l\}}{|\mathcal{X}_l|}$$

where $\pi_l > 0$ and $\sum_{l=1}^{k} \pi_l = 1$.

We will use non-informative priors for c, $\pi = (\pi_1, \ldots, \pi_k)$ and the error variance σ^2. The prior density of c will be specified as

$$p(c) = \frac{1}{(c_+ - c_-)} \mathbf{1}\{c \in [c_-, c_+]\}$$

while the prior density of π is

$$p(\pi) = \frac{1}{\text{vol}(D)} \mathbf{1}\{\pi \in D\},$$

where

$$D = \Big\{\pi \in \mathbb{R}^k : \pi_l > 0, \sum_{l=1}^{k} \pi_l = 1\Big\}.$$

The prior density of σ^2 will be of the form

$$p(\sigma^2) = \frac{1}{(\sigma_+ - \sigma_-)} \mathbf{1}\{\sigma \in [\sigma_-, \sigma_+]\}.$$

5.2 The likelihood model

Let the data be denoted by

$$z = \{z_{tx} : t = t_1, \ldots, t_m, x \in \mathcal{X}\}.$$

Then, the conditional density of z given c, π, ψ_0 and σ is

$$p(z|\psi_0, \sigma) = [2\pi\sigma^2]^{-Nm/2} \exp\Big(- \frac{1}{2\sigma^2} \|z - f(\psi_0)\|^2 \Big), \tag{3}$$

where

$$\|z - f(\psi_0)\|^2 = \sum_{t,x} \Big(z_{tx} - \sum_{[t_i, x_i; \theta_{i0}, \theta_{i1}\theta_{i2}] \in \psi_0} f_{tx}(t_i, x_i; \theta_{i0}, \theta_{i1}, \theta_{i2}) \Big)^2.$$

This is the simplest choice of model, see also [20] and references therein. Note that (3) does not depend on c and π.

5.3 Posterior simulation

The posterior density will be of the following form

$$p(c, \pi, \sigma, \psi_0|z) \propto p(c)p(\pi)p(\sigma^2)p(\psi_0|c, \pi)p(z|\psi_0, \sigma)$$

since the conditional density of ψ_0 given c, π and σ only depends on c and π and the conditional density of z given the remaining variables only depends on ψ_0 and σ. For the simulation from the posterior density we use a fixed scan Metropolis within Gibbs algorithm where in each scan c, π, σ and ψ_0 are updated in turn. For a detailed description of algorithms of this kind, see [24]. The full conditional for c is a Gamma distribution with restricted range while for $k > 2$ the full conditional of π is a Dirichlet distribution. The full conditional of σ^2 is an inverse Gamma distribution with restricted range.

Finally, we need to simulate from

$$p(\psi_0|c, \pi, z) \propto c^{n(\psi_0)} \prod_{l=1}^{k} \pi_l^{n_l(\psi_0)} \exp\Big(-\frac{1}{2\sigma^2}\|z - f(\psi_0)\|^2\Big).$$

Note that this is in fact a pairwise interaction density. The point process is simulated using a birth, death and move algorithm as described in Chapter 7 of [23].

5.4 An example

We consider here shortly a Bayesian analysis of a fMRI data set analyzed in [3] by ICA analysis and illustrated in Fig. 1. In the Bayesian analysis performed here, the values of $\theta_\star$ and σ^2 were fixed and equal to empirically assessed values. In [3], evidence was found of a resting state network involving three regions of the brain slice, the left and right motor cortices and a middle region. Those regions are delineated in Fig. 3. In Fig. 4, we show the estimated two-dimensional posterior density of time points of activation for pairs of regions from Fig. 3. All estimated correlations are positive and significantly different from zero.

In Fig. 5, we show examples of observed time series and their estimated temporal activation.

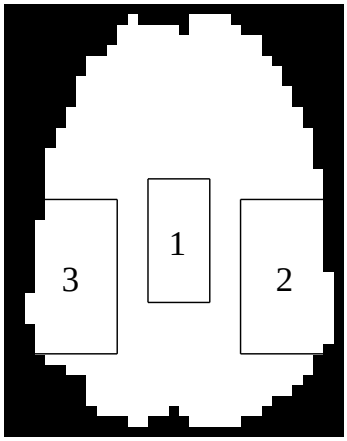

Figure 3: Delineation of the three regions of interest, $\mathcal{X}_1$, a middle region, $\mathcal{X}_2$ that includes the left motor cortex, and $\mathcal{X}_3$ that includes the right motor cortex.

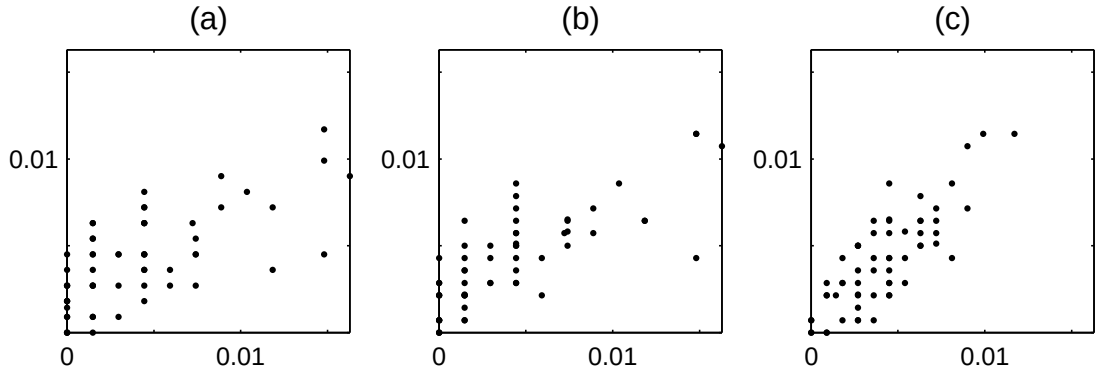

Figure 4: Two-dimensional posterior densities of time points of activation for pairs of regions delineated in Fig. 3. Regions $\mathcal{X}_1$ and $\mathcal{X}_2$ are shown in (a), $\mathcal{X}_1$ and $\mathcal{X}_3$ in (b) and $\mathcal{X}_2$ and $\mathcal{X}_3$ in (c). Each point represents a time interval of 4 seconds.

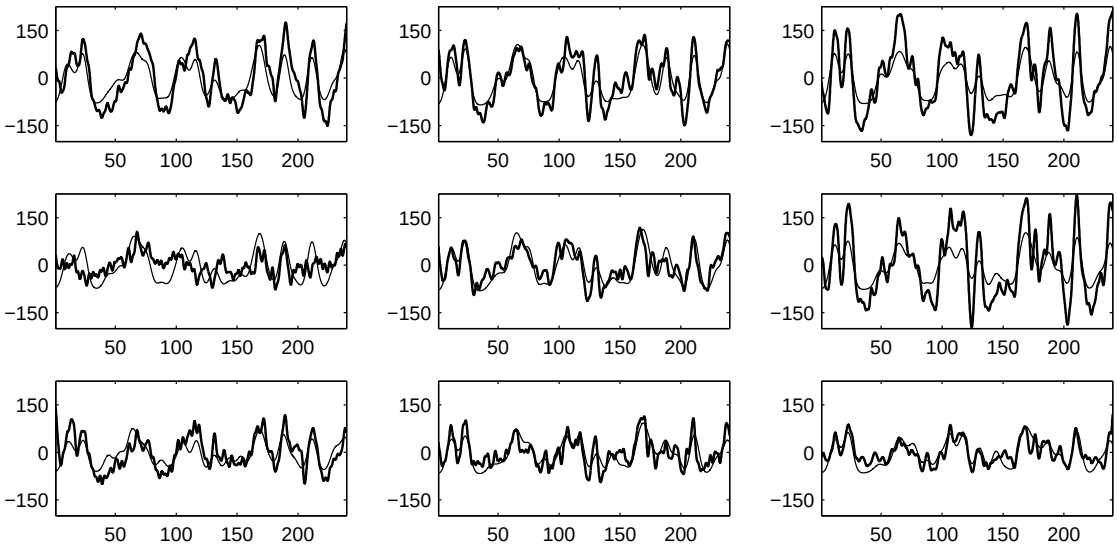

Figure 5: Time series from nine neighbouring voxels from the left motor cortex. In each plot, the thick line is the true, preprocessed time series for that voxel and the thin line is the estimated time series for the same voxel. The units on the x-axis are given in seconds.

6 Acknowledgements

This work was supported by the Danish National Science Research Council. The authors thank Christian F. Beckmann for sharing his data. Further, the authors are grateful for fruitful discussions with Klaus B. Bærentsen, Anders C. Green and Hans Stødkilde Jørgensen.

References

[1] Bartels, A. and Zeki, S.: *The Chronoartitecture of the Human Brain - Natural Viewing Conditions Reveal a Time-based Anatomy of the Brain.* NeuroImage **22** (2004), 419–433.

[2] Bartels, A. and Zeki, S.: *Brain Dynamics during Natural Viewing Conditions – A New Guide for Mapping Connectivity in Vivo.* NeuroImage **24** (2005), 339–349.

[3] Beckmann, C. F., DeLuca, M., Devlin, J. T. and Smith, S. M.: *Investigations into Resting-State Connectivity using Independent Component Analysis.* Phil. Trans. R. Soc. B **360** (2005), 1001–1013.

[4] Beckmann, C. F. and Smith, S. M.: *Tensorial Extensions of Independent Component Analysis for Multisubject FMRI Analysis.* NeuroImage **25** (2005), 294–311.

[5] Buckner, R. L., Snyder, A. Z., Sanders, A. L., Raichle, M. E. and Morris, J. C.: *Functional Brain Imaging of Young, Nondemented, and Demented Older Adults.* Journal of Cognitive Neuroscience **12** (2000), 24–34.

[6] Buxton, R. B., Uludağ, K., Dubowitz, D. J. and Liu, T. T.: *Modelling the Hemodynamic Response to Brain Activation.* NeuroImage **23** (2004), 220–233.

[7] De Luca, M., Beckmann, C. F., De Stefano, N., Matthews, P. M. and Smith, S. M.: *FMRI Resting State Networks Define Modes of Long-distance Interactions in the Human Brain.* NeuroImage **29** (2006), 1359–1367.

[8] Fox, M. D., Snyder, A. Z., Vincent, J. L., Corbetta, M., Van Essen, D. C. and Raichle, M. E.: *The Human Brain is Intrinsically Organized into Dynamic, Anticorrelated Functional Networks.* PNAS **102** (2005), 9673–9678.

[9] Friston, K.: *Modes or Models: a Critique on Independent Component Analysis for FMRI.* Trends in Cognitive Sciences **2** (1998), 373–375.

[10] Genovese, C. R.: *A Bayesian Time-Course Model for Functional Magnetic Resonance Imaging Data. With Discussion and a Reply by the Author.* J. Amer. Statist. Assoc. **95** (2000), 691–719.

[11] Giuliani, M.: *Selected Problems in Modelling.* Computer Press, Prague 2005.

[12] Gössl, C., Auer, D. P. and Fahr, L.: *Bayesian Spatiotemporal Inference in Functional Magnetic Resonance Imaging.* Biometrics **57** (2001), 554–562.

[13] Greicius, M. D., Krasnow, B., Reiss, A. L. and Menon, V.: *Functional Connectivity in the Resting Brain: a Network Analysis of the Default Mode Hypothesis.* PNAS **100** (2003), 253–258.

[14] Greicius, M. D. and Menon, V.: *Default-mode Activity during a Passive Sensory Task: Uncoupled from Deactivation but Impacting Activation.* Journal of Cognitive Neuroscience **16** (2004), 1484–1492.

[15] Greicius, M. D., Srivastava, G., Reiss, A. L. and Menon, V.: *Default-mode Network Activity Distinguishes Alzheimer's Disease from Healthy Aging: Evidence from Functional MRI.* PNAS **101** (2004), 4637–4642.

[16] Hartvig, N.: *A Stochastic Geometry Model for Functional Magnetic Resonance Imaging Data.* Scand. J. Statist. **29** (2002), 333–353.

[17] Hochstein, S. and Ahissar, M.: *View from the Top: Hierarchies and Reverse Hierarchies in the Visual System.* Neuron **36** (2002), 791–804.

[18] Houston, W.: *Unexpected Simulation Problem.* Appl. Math. **44** (1999), 267–276.

[19] Jensen, E. B. V. and Thorarinsdottir, T. L.: *A Spatio-temporal Model for FMRI Data - With a View to Resting State Networks.* Submitted.

[20] Lund, T. E., Madsen, K. H., Sidaros, K., Luo, W.-L. and Nichols, T. E.: *Non-white Noise in FMRI: Does Modelling have an Impact?* NeuroImage **29** (2006), 54–66.

[21] McKeown, M. J., Hansen, L. K. and Sejnowski, T. J.: *Independent Component Analysis of Functional MRI: What is Signal and What is Noise?* Current Opinion in Neurobiology **13** (2003), 620–629.

[22] Molchanov, I.: *Statistics of the Boolean Model for Practitioners and Mathematicians.* John Wiley & Sons, Chichester (1997).

[23] Møller, J. and Waagepetersen, R. P. : *Statistical Inference and Simulation for Spatial Point Processes.* Chapman & Hall/CRC, New York (2004).

[24] Robert, C.P. and Casella, G: *Monte Carlo Statistical Methods, 2nd Edition.* Springer, New York (2004).

[25] Smith, S. M., Jenkinson, M., Woolrich, M. W., Beckmann, C. F., Behrens, T. E. J., Johansen-Berg, H., Bannister, P. R., De Luca, M., Drobnjak, I., Flitney, D. E., Niazy, R. K., Saunders, J., Vickers, J., Zhang, Y., De Stefano, N., Brady, J. M. and Matthews, P. M.: *Advances in Functional and Structural MR Image Analysis and Implementation as FSL.* NeuroImage **23** (2004), 208–219.

[26] Woolrich, M. W., Jenkinson, M., Brady, J. M. and Smith, S. M.: *Fully Bayesian Spatio-temporal Modeling of FMRI Data.* Transactions of Medical Imaging **23** (2004), 213–231.